Bioorganic & Medicinal Chemistry Letters 27 (2017) 3851–3855

Contents lists available at ScienceDirect

Bioorganic & Medicinal Chemistry Letters

journal homepage: www.elsevier.com/locate/bmcl

Discovery of novel dengue virus entry inhibitors via a structure-based approach

Emilse S. Leal [a,f], M. Gabriela Aucar [b,c,f], Leopoldo G. Gebhard [d], Nestor G. Iglesias [d], María J. Pascual [e], Juan J. Casal [a], Andrea V. Gamarnik [d], Claudio N. Cavasotto [b,*], Mariela Bollini [a,*]

[a] Laboratorio de Química Medicinal, Centro de Investigaciones en Bionanociencias (CIBION)-CONICET, Godoy Cruz 2390, Ciudad de Buenos Aires, Argentina
[b] Laboratory of Computational Chemistry and Drug Design, Instituto de Investigación en Biomedicina de Buenos Aires (IBioBA) – CONICET – Partner Institute of the Max Planck Society, Godoy Cruz 2390, Ciudad de Buenos Aires, Argentina
[c] Instituto de Modelado e Innovación Tecnológica, CONICET, and Departamento de Fisica, FCENA-UNNE, Avda. Libertad 5460, Corrientes, Argentina
[d] Fundación Instituto Leloir-CONICET, Av. Patricias Argentinas 435, Ciudad de Buenos Aires, Argentina
[e] Instituto de Investigaciones Biotecnológicas, Universidad Nacional de San Martín, CONICET, Av. 25 de Mayo y Francia, San Martín, Prov. de Buenos Aires, Argentina

ARTICLE INFO

Article history:
Received 19 May 2017
Revised 15 June 2017
Accepted 19 June 2017
Available online 23 June 2017

Keywords:
Envelope protein
Structure-based drug design
Virtual screening
Anti-dengue drugs
Molecular dynamics

ABSTRACT

Dengue is a mosquito-borne virus that has become a major public health concern worldwide in recent years. However, the current treatment for dengue disease is only supportive therapy, and no specific antivirals are available to control the infections. Therefore, the need for safe and effective antiviral drugs against this virus is of utmost importance. Entry of the dengue virus (DENV) into a host cell is mediated by its major envelope protein, *E*. The crystal structure of the *E* protein reveals a hydrophobic pocket occupied by the detergent *n*-octyl-β-D-glucoside (β-OG) lying at a hinge region between domains I and II, which is important for the low-pH-triggered conformational rearrangement required for fusion. Thus, the *E* protein is an attractive target for the development of antiviral agents. In this work, we performed prospective docking-based virtual screening to identify small molecules that likely bind to the β-OG binding site. Twenty-three structurally different compounds were identified and two of them had an EC_{50} value in the low micromolar range. In particular, compound **2** (EC_{50} = 3.1 μM) showed marked antiviral activity with a good therapeutic index. Molecular dynamics simulations were used in an attempt to characterize the interaction of **2** with protein *E*, thus paving the way for future ligand optimization endeavors. These studies highlight the possibility of using a new class of DENV inhibitors against dengue.

Dengue virus (DENV) is the most prevalent mosquito-borne viral pathogen and has become a major public health concern worldwide. Presently, dengue is endemic in 112 countries around the world.[1] Mostly in tropical and subtropical areas, each year 50–100 million individuals are infected with DENV resulting in nearly 500,000 severe illnesses and 25,000 deaths.[2,3] Four distinct serotypes (DENV1-4) of the virus are the major contributors in circulation of DENV in the world population.[4] Although the number of dengue cases increases every year, there are no approved therapeutics available for the treatment of these infections.

DENV belongs to the flavivirus genus of the *Flaviviridae* family of positive-sense single-stranded RNA viruses.[5,6] The RNA genome encodes ten proteins; three of them (the so-called Capsid, Membrane and Envelope proteins) are structural proteins that are present in the infectious virus particle, composed of a lipid bilayer that anchors envelope and membrane proteins, surrounding the viral RNA complexed with the capsid protein. The other seven are nonstructural proteins (i.e.; NS1, NS2A, NS2B, NS3, NS4A, NS4B, and NS5) involved in amplifying the viral genome once the virus reaches the cytoplasm of the cell.[7] During viral morphogenesis, the capsid protein recruits the viral RNA genome on the cytosolic face of the endoplasmic reticulum (ER), and the assembled nucleocapsid buds into the ER lumen acquiring a coat that contains the Envelope (*E*) glycoprotein and the precursor Membrane protein, prM. Then, the particle passes through the secretory pathway, where a furin-like protease cleaves prM to M in a late *trans*-Golgi compartment.[8] The cleavage releases a constraint on the *E* glycoprotein and primes the particle for low-pH-triggered membrane fusion. The *E* glycoprotein is a major component of the virion surface and plays an important role in binding to the host receptor, drives viral fusion, and induces immunogenic response in host cell.[9,10]

* Corresponding authors.
E-mail addresses: cnc@cavasotto-lab.net, ccavasotto@ibioba-mpsp-conicet.gov.ar (C.N. Cavasotto), mariela.bollini@cibion.conicet.gov.ar (M. Bollini).
[f] These authors equally contributed to this work.

http://dx.doi.org/10.1016/j.bmcl.2017.06.049
0960-894X/

The crystal structure of the DENV *E* protein reveals a hydrophobic pocket occupied by the detergent *n*-octyl-β-D-glucoside (β-OG) lying at a hinge region between domains I and II of the protein, which is important for the low-pH-triggered conformational rearrangement required for membrane fusogenic activity. Therefore, the β-OG binding site was proposed as an appropriate target for developing small-molecule inhibitors of virus-host membrane fusion process.[11–14]

The available structural data of the DENV *E* opened up the possibility to identify antiviral agents interfering with the early steps of DENV infection. In this work, we undertook a multistep hierarchical prospective structural-based virtual screening (SBVS) strategy targeting the β-OG hydrophobic binding site of the solved crystal structure of protein *E* (PDB code: 1OKE) to identify novel entry inhibitors with improved potency and efficacy against *E*. Docking-based virtual screening was performed using approximately 110,000 small-molecules from the Maybridge database using the ICM software, which proved successful for finding hits on several other targets.[15–18] The screening protocol began with an ADME filter,[19] in order to retain only potentially non-toxic and druggable molecules, which were subjected to two independent high-throughput docking (HTD) screenings, where the best score per molecule was kept.[20] The top ranked 500 molecules were manually inspected using the following criteria: (i) docking pose overlapping with the co-crystallized β-OG ligand, (ii) interaction with binding site amino acids, (iii) scaffold diversity, (iv) commercial availability, and (v) synthetic tractability for potential modifications. All molecules containing unwanted structural features were removed such as those with readily hydrolyzable and/or highly electrophilic functional groups. Finally, 23 compounds were taken into consideration for in vitro studies (Scheme S1, Supplementary Information) and were either purchased or synthesized. In particular, compound **2** was prepared and the synthetic route is shown in Scheme 1. The quinazoline ring was installed by condensing aniline **6** with formamide at 150 °C. Heating of compound **7** in excess of thionyl chloride afforded 4-chloro quinazoline **8**. The nucleophilic displacement of chlorine in compound **8** by 2-amino-2-pyridinol proceeded in the presence of Cs_2CO_3 in DMF at 100 °C in a good yield, and produced the intermediate **9**. Finally, the target compound **2** was obtained by amidation with 5-(pyridin-2-yl)thiophene-2-carboxylic acid mediated by BOP [1-benzotriazolyl-oxy-tris-(dimethylamino)phosphonium-hexafluoro-phosphate] as a coupling reagent (Scheme 1).

The identities of the purchased compounds and compound 2 were verified by NMR and mass spectrometry, and the purity was found to be at least 95% by HPLC.

Antiviral activity was next assessed using a reporter DENV assay based on the measurement of luciferase expression from a recombinant fully functional virus bearing a luciferase coding sequence in the context of the viral genome.[21,22] After infection of cells in culture with the reporter DENV, luciferase activity first peaks at 8 h as a result of translation of the incoming genomes, reflecting virus entry into the host cells. At 24 h post infection, amplification of the genome by the viral polymerase results in an increase in luciferase activity that reflects virus RNA synthesis. Luciferase activity was measured at 8 and 24 h post infection with the reporter DENV in untreated or treated cells with each of the 23 compounds identified in the virtual screening. The results showed that 5 hits displayed antiviral activity against DENV (Fig. 1, Table 1). Compounds **2**, **5** and **4** showed marked antiviral inhibition at 8 h post infection with a good selectivity index. Compounds **1** and **3** showed moderate inhibitory activities and no cytotoxicity was detected at 100 μM. In order to examine the selective antiviral potential of the compounds identified in the virtual screening, we tested these compounds against bovine viral diarrhea virus (BVDV), another member of the Flaviviridae family. None of them

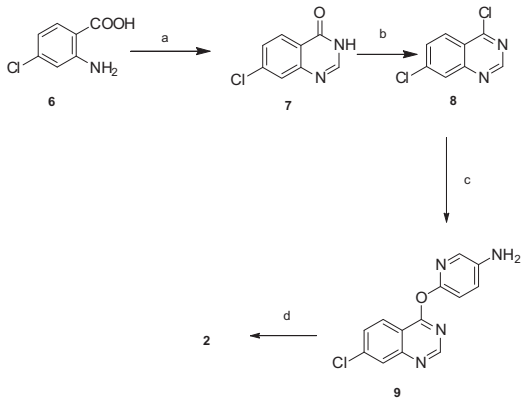

Scheme 1. Synthetic route for the preparation of compound **2**. Reagents and conditions (a) Formamide, 150 °C; (b) $SOCl_2$, reflux, 8 h; (c) 5-aminopyridin-2-ol, Cs_2CO_3, DMF, 100 °C, 24 h; (d) 5-(Pyridin-2-yl)thiophene-2-carboxylic acid, BOP, DIPEA, rt, overnight.

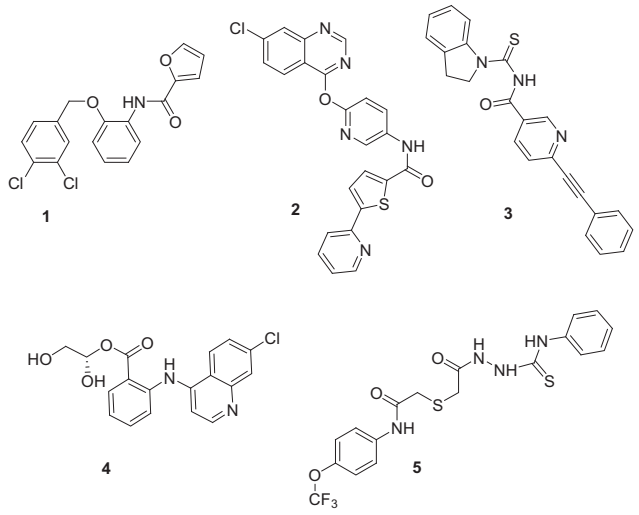

Fig. 1. Chemical structures of novel anti-dengue inhibitors.

Table 1
In vitro antiviral effect, cytotoxicity and selectivity of compounds identified (as hits) from the virtual screening.

Compound	EC_{50} (μM)[a]		CC_{50} (μM)[b]	SI[c] (DENV)
	DENV-2[d]	BVDV		
1	22.7 ± 1.2	>50	>100	>5
2	3.1 ± 1.1	>50	>100	>32
3	28.7 ± 1.0	>50	>100	>4
4	10.8 ± 1.1	>50	>100	>9
5	5.1 ± 0.9	>50	>100	>20

[a] EC50: 50% effective concentration.
[b] CC50: 50% cytotoxic concentration.
[c] SI: selectivity index.
[d] 8 h post infection.

demonstrated significant antiviral activity at 50 μM. Taken together, our results suggested that active compounds interfere with early steps of the DENV life cycle, most likely during viral entry.

To better characterize the likely interaction of the new ligands with protein *E*, and to explore the role of water molecules (cf. Ref. 23) (omitted during the docking stage), that might be involved in mediating protein-ligand interaction, we performed 100 ns MD simulation on the most active compound (**2**). The docked pose of

compound **2** was used as the initial conformation. It can be observed that the protein remains stable throughout the simulation (Fig. S2). The predicted binding pose of **2** within the *E* protein is displayed in Fig. 2a.

The 4-substituted 7-chloro-quinazoline moiety remains exposed to the solvent, while the pyridine attached to it makes contacts with Thr48, Glu49, Leu135, Gln271 and Leu277 (Fig. 2b); the system is further stabilized by a dynamic moderate hydrogen bond between the pyridine N and the HN of Ala50, exhibiting an interatomic distance below 2.5 Å during half of the last 50 ns simulation. The O in the amide is intermittently exposed to the solvent through a narrow channel. Several water molecules were found throughout the simulation within the binding site, bridging the interaction of the ligand with the protein. A water molecule with

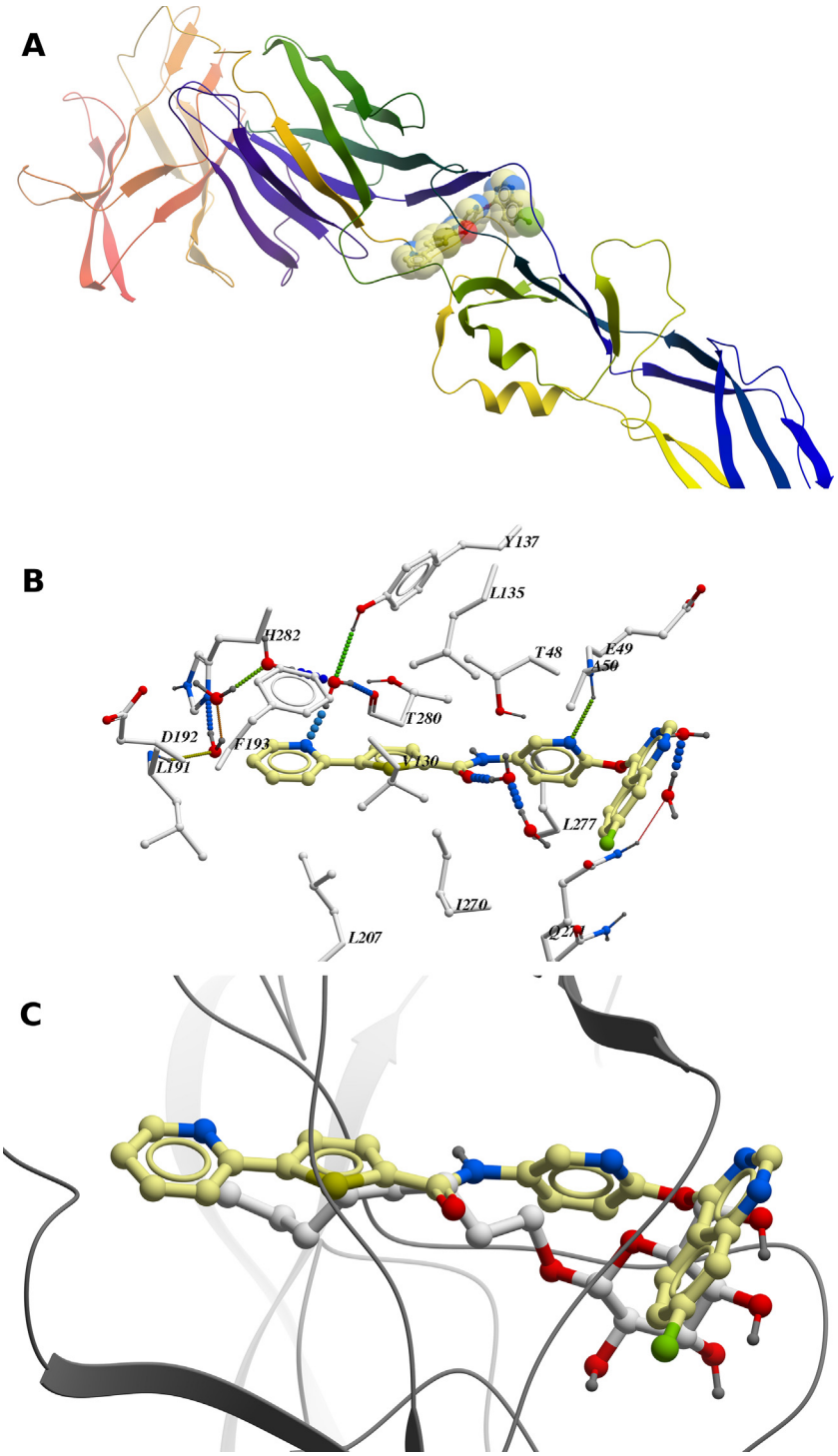

Fig. 2. Predicted interaction of compound **2** within the *E* protein β-OG binding site, extracted from the molecular dynamics simulation. (A) Ribbon representation of protein *E* with compound **2** within the binding site (B). Interaction of **2** with the binding site amino acids and water molecules. For simplicity, backbone nitrogens, carbonyl oxygens are not displayed, except when interacting directly with **2**. Only polar hydrogens are shown. Hydrogen bonds are shown as a line of colored spheres. Color code: **2**, yellow carbons; DENV *E* carbons, white; oxygens, red; nitrogens, blue; sulphur, green; polar hydrogens, dark gray. (C) Superposition of **2** with the β-OG ligand within the binding site. Color code: DENV *E* protein, gray ribbon; β-OG, white carbons. Figure prepared with ICM, (MolSoft LLC, La Jolla, CA).

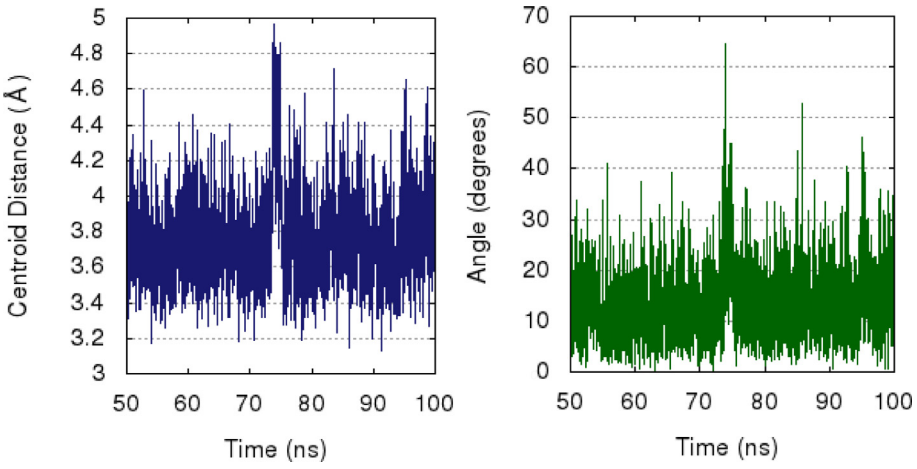

Fig. 3. Plane angles (left panel) and ring centroid distances (right panel) for the π-π interaction between Phe193 and the terminal pyridine moiety of compound **2**.

Table 2
Calculated pharmacological characteristics, experimental solubility and stability for active compounds.

Compound	EC_{50} (μM)[a]	QlogP[b]	QlogS[c]	QPCaco[d]	#met[e]	Aqueous solubility[f] μg/mL pH			PBS stability (h)
						2.0	6.4	7.4	
2	3.1	4.2	−4.5	785.8	4	12.7	10.1	2.9	>48
4	10.8	3.9	−5.2	520.5	5	48.3	32.1	6.1	>48
5	5.1	3.7	−5.2	1735.6	3	8.2	13.1	1.2	>48

[a] EC_{50} (μM) was calculated from dose–response curves by Prism software. The results represent the average of two or more independent experiments.
[b] Octanol/water partition coefficient (log Po/w).
[c] aqueous solubility.
[d] Caco-2 cell permeability.
[e] Number of metabolites.
[f] Experimental solubility at pH 2, 6.4, 7.4. Reference values at pH 6.4 for piroxicam 7.3 μg/mL and efavirenz 68.3 μg/mL. Values are means of two independent experiments, each running triplicate.

almost 100% occupancy in the last 50 ns makes hydrogen bonds with the N of the terminal pyridine, the hydroxyl group of Tyr137, the carboxylic O of Thr280, and another water molecule, which belongs to a small conserved cluster of three buried water molecules that also interact with the HN of Leu 191 and His282, the carboxylic O of Thr189 and the side chain of His282. A stable π-π interaction between the terminal pyridine ring and Phe193 is also observed throughout the simulation, with an average ring centroid distance of 3.7 Å and an average planes angle of 14° (Fig. 3). The 2-(thiophen-2-yl) pyridine moiety is stabilized by hydrophobic contacts with Val130, Leu191, Asp192, Leu207, Ile270, Phe279, and Thr280. It should be stressed that compound **2** overlaps very well with co-crystallized ligand β-OG (Fig. 2c). The predicted protein-ligand interaction pattern is in line with recent models.[14]

Finally, the pharmacologic characteristics of drug candidates were predicted using QikProp program[19,24] and are summarized in Table 2. QikProp generates physically relevant descriptors and uses them to perform ADMET predictions. A compound is viewed as potentially problematic if it does not satisfy a "rule-of-three": predicted logS > −6.0, PCaco > 30 nm/s, and maximum number of primary metabolites of six. The most potent compounds reported here compare favorably with all these limits.

In humans, the pH value in stomach is 1–2, while in small intestine it is 5–7. Because compound solubility often depends on pH in solution, it is important to consider different pH buffers. Taking into account the relevance of drug solubility, in vivo absorption and distribution, we tested the in vitro solubility and stability in PBS media for active compounds **2**, **4**, **5** at pH 2.0, 6.4, and 7.4. The solubility data are summarized in Table 2; all compounds showed good solubility and are well inside the range normally observed for oral drugs, 4–4000 μg/mL[24] corresponding to an S of 10^{-2}–10^{-5} M for compounds with a molecular weight of 400. The ClogP values for the listed compounds are between 3 and 5, which are in the normal range of 0–5 for oral drugs.[25] The aqueous solubility pattern of the assayed compounds was similar to the predicted solubility.

Compounds **2**, **4** and **5** showed low to moderate solubility ranging from 1 to 10 μg/mL at pH 7.4. However, these compounds are more soluble at pH 2.0 and pH 6.4.

All the compounds also had a reasonable stability in buffer (>48 h), so no intrinsic stability issues were expected.

Here, we have described a prospective structure-based drug discovery approach to identify novel and potent inhibitors of DENV entry targeting protein *E*. We performed a multistep hierarchical high-throughput docking of the 110,000 Maybridge compounds library, leading to the identification of the quinazoline hit **2** with an EC_{50} of 3 μM, and compound **5** with an EC_{50} of 5 μM, both with a good therapeutic index. Molecular docking for compound **5** and molecular dynamics approaches for **2** predicted strong interactions of both compounds with the key amino acids in the β-OG binding pocket of protein *E* that are crucial for membrane fusion to deliver the viral genome in the cytoplasm of the infected cell, in agreement with earlier works.[13,14] In summary, we have provided novel DENV inhibitors that interfere early during infection, stablishing a platform for the development of new and more potent antivirals against this important human pathogen.

Computational methods

High-throughput docking

All simulations were based on the crystal structure of the ectodomain of the envelope glycoprotein from dengue virus type 2 bound to the detergent *n*-octyl-β-D-glucoside (β-OG) (PDB 1OKE).[10] The molecular system was described in terms of torsional coordinates using the ECEPP/3 force field[26] as implemented in the ICM program (version 3.7-2c, MolSoft LLC, La Jolla, CA)[27,28] The system was prepared in a similar fashion as in earlier works[29–31] (further details are shown in Supplementary Information).

Molecular dynamics

MD simulations were performed using GROMACS v4.6 package[32,33] with the Amber99SB force field[34] for proteins. Force field parameters for small-molecules were obtained through the AnteChamber PYthon Parser inerfacE (ACPYPE)[35] using the GAFF[36] force field. After equilibration, the system was subjected to a 100 ns MD simulation at 310 K (further details are shown in Supplementary Information).

Acknowledgments

This work has been supported by the Agencia Nacional de Promoción Científica y Tecnológica, Argentina (PICT 2013-0078 and PICT 2014-1884 to MB; PICT 2014-3599 to CNC and MB), CONICET (PIP 2014 11220130100721 to MB and CNC), and FOCEM-Mercosur (COF 03/11).

MB thanks William Jorgensen for providing an academic license for QikProp software. CNC thanks Molsoft LLC for providing an academic license for the ICM program. The authors thank the National System of High Performance Computing (Sistemas Nacionales de Computación de Alto Rendimiento, SNCAD) and the Computational Centre of High Performance Computing (Centro de Computación de Alto Rendimiento, CeCAR) for granting use of their computational resources, and Diego Alvarez for technical help and critical discussion of the manuscript.

A. Supplementary data

Supplementary data associated with this article can be found, in the online version, at http://dx.doi.org/10.1016/j.bmcl.2017.06.049.

References

1. <http://www.who.int/mediacentre/factsheets/fs117/es/>.
2. Gubler DJ. *Trends Microbiol*. 2002;10:100–103.
3. Whitehead SS, Blaney JE, Durbin AP, Murphy BR. *Nat Rev Microbiol*. 2007;5:518–528.
4. Ligon BL. *Semin Pediatr Infect Dis*. 2005;16:60–65.
5. Wichapong K, Nueangaudom A, Pianwanit S, Sippl W, Kokpol S. *Trop Biomed*. 2013;30:388–408.
6. Murphy FA. In: Mahy BWJ, Van Regenmortel MHV, eds. *Encyclopedia of Virology*. 3rd ed. Oxford: Academic Press; 2008:140–148.
7. Yan Y, Li Y, Munshi S, et al. *Protein Sci*. 1998;7:837–847.
8. Plevka P, Battisti AJ, Junjhon J, et al. *EMBO Rep*. 2011;12:602–606.
9. Kuhn RJ, Zhang W, Rossmann MG, et al. *Cell*. 2002;108:717–725.
10. Modis Y, Ogata S, Clements D, Harrison SC. *Proc Natl Acad Sci USA*. 2003;100:6986–6991.
11. Poh MK, Yip A, Zhang S, et al. *Antiviral Res*. 2009;84:260–266.
12. Wang QY, Patel SJ, Vangrevelinghe E, et al. *Antimicrob Agents Chemother*. 2009;53:1823–1831.
13. Behnam MAM, Nitsche C, Boldescu V, Klein CD. *J Med Chem*. 2016.
14. Jadav SS, Kaptein S, Timiri A, et al. *Bioorg Med Chem Lett*. 2015;25:1747–1752.
15. Cavasotto CN, Orry AJW, Murgolo NJ, et al. *J Med Chem*. 2008;51:581–588.
16. Cavasotto CN, Ortiz MA, Abagyan RA, Piedrafita FJ. *Bioorg Med Chem Lett*. 2006;16:1969–1974.
17. Chan F-Y, Sun N, Neves MAC, et al. *J Chem Inf Model*. 2013;53:2131–2140.
18. Sun N, Chan F-Y, Lu Y-J, et al. *PLoS One*. 2014;9:e97514.
19. Jorgensen WL. QikProp, v 3.0. Schrödinger LLC.
20. Cavasotto CN, Abagyan RA. *J Mol Biol*. 2004;337:209–225.
21. Mondotte JA, Lozach P-Y, Amara A, Gamarnik AV. *J Virol*. 2007;81:7136–7148.
22. Kato F, Hishiki T. *Viruses*. 2016;8:122.
23. Spyrakis F, Cavasotto CN. *Arch Biochem Biophys*. 2015;583:105–119.
24. Jorgensen WL, Duffy EM. *Adv Drug Deliv Rev*. 2002;54:355–366.
25. Jorgensen WL. *Acc Chem Res*. 2009;42:724–733.
26. Nemethy G, Gibson KD, Palmer KA, et al. *J Phys Chem*. 1992;96:6472–6484.
27. Abagyan R, Totrov M, Kuznetsov D. *J Comput Chem*. 1994;15:488–506.
28. Neves MAC, Totrov M, Abagyan RJ. *Comput Aided Mol Des*. 2012;26:675–686.
29. Petrov RR, Knight L, Chen SR, et al. *Eur J Med Chem*. 2013;69:881–907.
30. He W, Elizondo-Riojas MA, Li X, et al. *Biochemistry*. 2012;51:8321–8323.
31. Monti MC, Casapullo A, Cavasotto CN, et al. *Chem Eur J*. 2009;15:1155–1163.
32. Berendsen HJC, van der Spoel D, van Drunen R. *Comput Phys Commun*. 1995;91:43–56.
33. Hess B, Kutzner C, van der Spoel D, Lindahl E. *J Chem Theory Comput*. 2008;4:435.
34. Hornak V, Abel R, Okur A, Strockbine B, Roitberg A, Simmerling C. *Proteins*. 2006;65:712–725.
35. Wang J, Wolf RM, Caldwell JW, Kollman PA, Case DA. *J Comput Chem*. 2004;25:1157–1174.
36. Beveridge DL, DiCapua FM. *Annu Rev Biophys Biophys Chem*. 1989;18:431–492.